Rare earth element analysis in natural waters by multiple isotope dilution - sector field ICP-MS.

Tristan C. C. Rousseau,[*a] Jeroen E. Sonke,[a] Jerome Chmeleff,[a] Frederic Candaudap,[a] François Lacan,[b] Geraldo Boaventura[c], Patrick Seyler[a] and Catherine Jeandel[b].

[*]corresponding author: tristanrousseau@yahoo.fr
[a]: *GET, Université de Toulouse, CNRS, IRD, CNES, 14 Avenue Edouard Belin, F-31400 Toulouse, France, 14 Avenue Edouard Belin, F-31400 Toulouse, France*
[b]: *LEGOS, Université de Toulouse, CNRS, IRD, CNES, 14 Avenue Edouard Belin, F-31400 Toulouse, France*
[c]: *Universidade De Brasilia, UNB, LAGEQ, Campus universitario Darcy Ribeiro 70.910-900 Brasilia -DF -*

Supplementary Information

Contents:

1. Spike calibration on MC-ICPMS

Isotopically enriched REE spikes were originally obtained from Oak Ridge National Laboratory in the 1990's and dissolved and stored in 10% HNO3 at 4°C. We calibrated these spike mother solutions for their concentration and isotopic composition (IC) in 2010 with a Thermo-Finingan Neptune MC-ICP-MS at the Midi-Pyrenees Observatory (Toulouse, France).

1.1. Cup configuration, mass bias and interferences corrections

MC-ICP-MS cup configurations

Five different MC-ICP-MS cup configurations were used for the 10 enriched REE spike calibrations (Table S1). La, Ce, Nd, Eu, Er and Lu were analyzed in static mode and Sm, Gd, Dy, Yb in dynamic mode in order to be able to measure all REE isotopes and isobaric interferences.

Table S1: A total of five MC-ICP-MS cup configurations were used to calibrate the single REE enriched spike mother solutions. Ratios used for exponential law mass bias correction and for reverse isotope dilution are indicated in the last two columns. Interfered isotopes are marked with a star, third isotopes used for isobaric corrections are marked with a circle note that ^{142}Nd could not be corrected for the minor isobaric interference ^{142}Ce.

	Main Cup Config.	L4	L3	L2	L1	C	H1	H2	H3	H4	Ratios used for Mass Biass Corection	Ratios used forReverse Isotope Dilution
La	1	^{136}Ce	^{137}Ba	^{138}Ce*	^{139}La	^{140}Ce	^{141}Pr	^{142}Ce	^{144}Nd	^{147}Sm	^{140}Ce/^{142}Ce*	^{138}La/^{139}La
Ce	1	^{136}Ce*	^{137}Ba°	^{138}Ce*	^{139}La	^{140}Ce	^{141}Pr	^{142}Ce	^{144}Nd°	^{147}Sm	^{140}Ce/^{142}Ce*	^{136}Ce/^{140}Ce
Nd	1	*^{142}Nd**	^{143}Nd*	^{144}Nd*	^{145}Nd	^{146}Nd	^{147}Sm°	^{148}Nd*	^{150}Nd*		^{145}Nd/^{143}Nd	^{146}Nd/^{145}Nd
Sm Mode1	2	^{144}Sm	^{145}Nd	^{146}Nd°	^{147}Sm	^{148}Sm*	^{149}Sm	^{150}Sm*	^{152}Sm*	^{155}Gd	^{147}Sm/^{149}Sm	^{147}Sm/^{149}Sm
Sm Mode2	2	^{149}Sm	^{150}Sm*	^{151}Eu	^{152}Sm*	^{153}Eu	^{154}Sm*	^{155}Gd°	^{157}Gd	^{160}Gd	^{152}Sm/^{149}Sm	
Eu	2	^{149}Sm	^{150}Sm	^{151}Eu	^{152}Sm	^{153}Eu	^{154}Sm	^{155}Gd	^{157}Gd	^{160}Gd	^{151}Eu/^{153}Eu	^{151}Eu/^{153}Eu
Gd Mode1	2	^{149}Sm°	^{150}Sm	^{151}Eu	^{152}Gd*	^{153}Eu	^{154}Gd*	^{155}Gd°	^{157}Gd	^{160}Gd°	^{155}Gd/^{157}Gd	^{155}Gd/^{157}Gd
Gd Mode2	2	^{152}Gd	^{153}Eu	^{154}Gd	^{155}Gd	^{156}Gd*	^{157}Gd	^{158}Gd*	^{160}Gd*	^{163}Dy°	^{155}Gd/^{157} Gd	
Dy Mode1	3	^{155}Dy	^{156}Gd*	^{157}Gd	^{158}Dy*	^{159}Tb	^{160}Dy*	^{161}Dy	^{163}Dy	^{166}Er	^{163}Dy/^{161}Dy	^{163}Dy/^{161}Dy
Dy Mode2	3	^{156}Dy*	^{157}Gd°	^{158}Dy*	^{159}Tb	^{160}Gd*	^{161}Dy	^{162}Dy*	^{164}Dy	^{167}Er°	^{162}Dy*/^{161}Dy	
Er	4	^{162}Er*	^{163}Dy°	^{164}Er*	^{165}Ho	^{166}Er	^{167}Er	^{168}Er*	^{170}Er*	^{173}Yb°	^{166}Er/^{167} Er	^{166}Er/^{167} Er
Yb Mode1	5	^{167}Er°	^{168}Er*	^{169}Tm	^{170}Er*	^{171}Yb	^{172}Yb	^{173}Yb	^{175}Lu	^{178}Hf	^{173}Yb/^{172}Yb	^{172}Yb/^{171}Yb
Yb Mode2	5	^{168}Yb	^{169}Tm	^{170}Yb°	^{171}Yb	^{172}Yb	^{173}Yb	^{174}Yb*	^{176}Yb*	^{179}Hf°	^{173}Yb/^{172}Yb	
Lu	5	^{171}Yb	^{172}Yb	^{173}Yb°	^{174}Yb	^{175}Lu	^{176}Lu*	^{177}Hf°	^{179}Hf	^{182}W	^{175}Lu/^{176}Lu*	^{175}Lu/^{176}Lu*

Instrumental mass bias

The MC-ICP-MS discriminates against the transmission of light isotopes relative to heavy isotopes. This is called mass bias, and requires to be corrected for. We did so by bracketing the pure spike and mixed spike/JMC solutions with natural abundance REE solutions. Since mass bias is concentration dependent, the REE bracketing solution had approximately the same concentrations (within 10%) as the pure spike and mixed spike/JMC solutions. Fractionation factors, f, were calculating using the exponential mass fractionation law:

$$f = \frac{Ln\left(\frac{r_{1/2}}{R_{1/2}}\right)}{Ln\left(\frac{M_1}{M_2}\right)} \quad \text{(Eq.S1)}$$

$R_{1/2:}$ true ratio of relative abundances between isotopes 1 et 2
$r_{1/2}$: measured ratio in Volts between isotope 1 and 2
M_1: atomic mass of isotope 1
M_2: atomic mass of isotope2

The ratios measured in the bracketed spike or mixed spike/JMC solutions are corrected using interpolated 'f' values from bracketing solutions.

$$r_{cor} = \frac{r_{mes}}{\left(\frac{M_1}{M_2}\right)^f} \quad \text{(Eq.S2)}$$

r_{mes}: Ratio between isotope 1 and 2 measured in the spike or JMC/spike mixed solutions
r_{cor}: Corrected Ratio between isotope 1 and 2

Isobaric Interference corrections

Isobaric interference corrections were made by subtracting the signal of an interference free isotope of the isobaric interfering one divided by its abundance multiplied by the interfering isotope abundance:

$$V_{1corr} = V_{1mes} - \frac{V_{3mes}}{A_3} * A_1 \quad \text{(Eq.S3)}$$

As there is also a mass bias between isotopes 1 and 3, it was taken into account using equations S1 and S2.

$$V_{1corr} = V_{1mes} - \left(\frac{M_1}{M_3} * \left(\frac{A_1}{A_3}\right)^f\right) * V_3 \text{ (Eq.S4)}$$

When the interfered isotope was necessary for mass bias calculation, the interfering isotope contribution was calculated iteratively, applying first a non-mass bias corrected isobaric interference correction. This allowed to calculate a first fractionation factor used to recalculate the interfering signal with Eq. S4 to finally calculate a more precise fractionation factor.

1.2. Enriched REE spike calibration

The relative abundances of REE isotopes in the enriched REE spike mother solutions were calculated as follows:

$$A^X M = \frac{1}{\left(\frac{\sum(A^y M)}{A^X M} + 1\right)} \quad \text{(Eq.S5)}$$

A^X_M: Relative abundance for the isotope X of element M
A^y_M: Relative abundances for the isotopes Y of the element M, excluding X
,as illustrated for Nd:

A^{142} Nd + A^{143} Nd + A^{144} Nd + A^{145} Nd + A^{147} Nd + A^{148} Nd + A^{150} Nd =1 (Eq.S6)

Dividing all terms by A^{143}_{Nd} and rearranging:

$$A^{143}Nd = \frac{1}{\left(\frac{\sum(A^{y}Nd)}{A^{143}Nd}+1\right)} \text{(Eq.S7)}$$

Abundance ratios in equation S7 were then substituted by the signal ratios in volts measured by MC-ICP-MS after blank, interference and mass bias corrections.

$$\hat{A}^{143}Nd = \frac{1}{\left(\frac{\sum(V^{y}Nd)}{V^{143}Nd}+1\right)} \text{(Eq.S8)}$$

$\hat{A}^{143}_{Nd}$: calculated abundance for ^{143}Nd in the spike
V^{y}_{Nd}: Signal in volts for the Y's atomic masses of the element M measured by MC-ICP-MS

All Nd isotope abundances in the spike could then be deduced, for ex. for ^{142}Nd:

$$\hat{A}^{142}Nd = \hat{A}143Nd * \frac{V^{142}Nd}{V^{143}Nd} \qquad \text{(Eq.S9)}$$

The spike's atomic masses were then determined using the measured relative abundances of isotopes in the spike and individual isotope atomic masses from:
NIST (http://www.nist.gov/pml/data/comp.cfm/)

$$MNd_{Spk=} \Sigma(\hat{A}^{x}_{Nd} * M^{x}_{Nd}) \qquad \text{(Eq.S10)}$$

MNd_{Spk}: Nd's Spike atomic mass calibrated with MC-ICP-MS
M^{x}_{Nd}: NIST isotope mass for the isotopes 'x'

Concentrations were determined by reverse isotope dilution (RID), which is achieved by mixing a commercial mono-elementary REE solution, with isotopes of natural relative abundances, with the corresponding enriched REE mother spike solution. We used commercial 1000 mg.kg^{-1} single REE solutions from the Johnson Matthey Company (JMC) that have a certified uncertainty of 0.3% RSD.

RID isotope pairs were chosen according to the relative abundances and the absence of isobaric interferences, when possible**.** The RID formula can be written as:

$$[REE]_{spk} = [REE]_{jmc} * \frac{\frac{W_{jmc}}{W_{spk}}}{\left(\frac{R_{spk}-R_m}{R_m-R_{nat}} * \frac{A2_{spk}}{A2_{nat}} * \frac{M_{nat}}{M_{spk}}\right)} \qquad \text{(Eq.S11)}$$

W_{jmc}: Mass in g of certified JMR REE solution mixed with the spike
W_{spk}: Mass in g of the spike solution
R_{spk}: Ratio of A_1/A_2 in the spike (determined during the IC calibration)
R_{nat}: Ratio of natural A_1/A_2
R_m: Corrected ratio of V_1/V_2 in the mixed solution measured by MC-ICP-MS

2. Optimum Spike/Sample mixing

The optimum spike to natural REE isotope ratios was determined for each REE using the uncertainty magnification factor formula:

$$M = \frac{(R_{nat} - R_{spk}) * R_{mix}}{(R_{mix} - R_{nat}) * (R_{spk} - R_{mix})} \qquad \text{(Eq.S12)}$$

R_{nat} and R_{spk} being constant, the function $M=f(R_{mix})$ has an uncertainty minimum for:

$$\frac{dM}{dR_{mix}} = 0 \qquad \text{(Eq.S13)}$$

The solution to Eq.S13 can be formulated for $R_{mix} = R_{mix_{ideal}}$ and corresponds to the ideal amount of spike/natural REE mixing:

$$R_{mix_{ideal}} = \sqrt{R_{spk} * R_{nat}} \qquad \text{(Eq.S14)}$$

Figure S1 illustrates the mixing between natural Nd and enriched ^{146}Nd spike for the ratio ^{146}Nd/^{145}Nd. The value for M decreases between the R_{nat} (2.07) and the $R_{mix_{ideal}}$ (19.63) corresponding to the underspiking zone and increases between $R_{mix_{ideal}}$ and R_{spk} (186.4) corresponding to the overspiking zone.

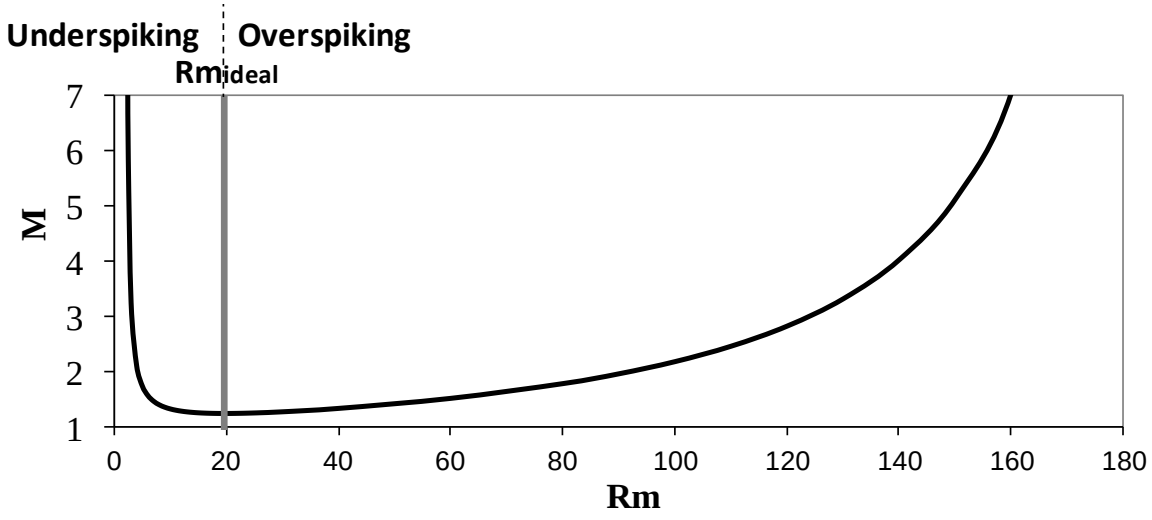

Figure S1: Uncertainty magnification factor 'M' as a function of the ^{146}Nd/^{145}Nd mixing ratio used for Nd isotope dilution.

In practice, the ideal amount of isotopic spikes were approximated using the reverse isotope dilution equation (Eq.S11) for a given sample [REE] and replacing R_m by $R_{mix_{ideal}}$. One difficulty is that added spike isotopes may themselves generate molecular and isobaric interferences. Therefore, simulations of ideally spiked samples were made numerically considering several plausible levels of plasma oxide and hydroxyde formation in order to

evaluate the magnitude of oxihydroxide interferences (ie: Ba and LREE on MREE and MREE on HREE) and isobaric interferences (ie: Ba, La, Ce and Yb, Lu, Hf).

After this optimization to limit isobaric and oxide interferences, a stock of mixed LREE spike and mixed HREE spike solutions was prepared. These stock solutions contain respectively 51ppb for La, 15ppb for Ce, 113 ppb for Nd, 48 ppb for Sm, 18 ppb for Eu and 92 ppb for Gd (mixed spike LREE) and 116 ppb for Dy, 65 ppb for Er, 41 ppb for Yb and 17 ppb for Lu (mixed spike HREE). Dilutions of those mother solutions were made to achieve 200µl to 1ml of spike aliquots when spiking samples. A SF-ICPMS mass spectrum of both HREE and LREE mixed spike solutions is reported in Figure S2.

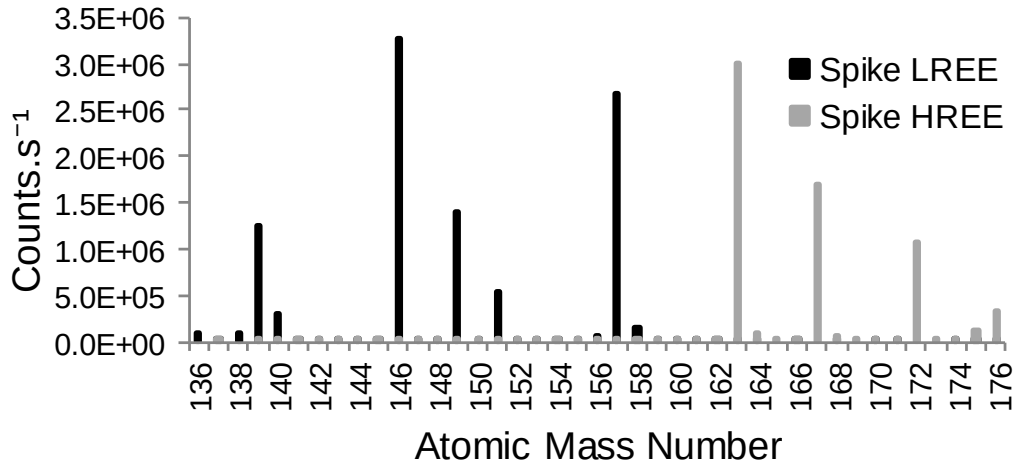

Figure S2: HREE (black) and LREE (grey) mixed spike mass spectrum measured with Thermo Element-XR coupled with the Aridus 2 desolvator.

The average dispersion of the uncertainty magnification factor 'M' obtained on the 19 samples analyzed in this study are reported in Figure S3. The grey line represents for each element the theoretical uncertainty magnification factor corresponding to an ideal proportion of sample/spike mixing and the boxplots represent the observed uncertainty magnification factor. Except for La and Lu which are overspiked on purpose all isotope/sample mixing proportions were close to ideal.

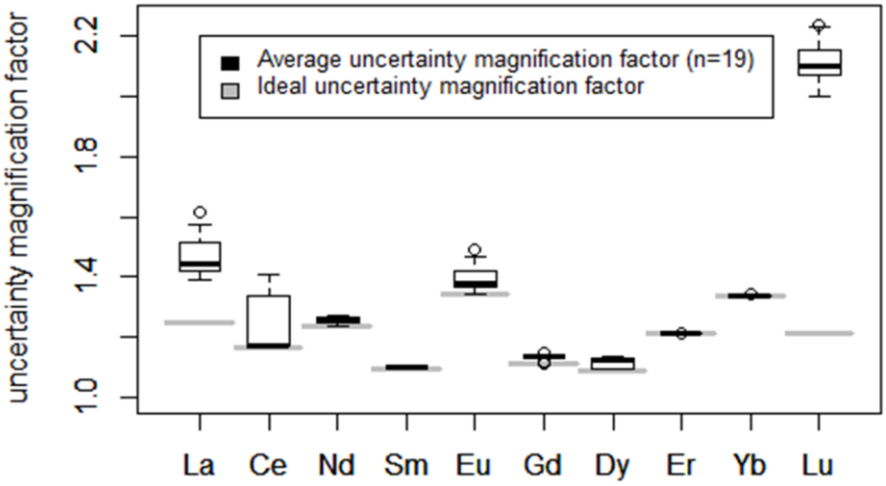

Figure S3: REE isotope dilution 'M' uncertainty magnification factors based on 19 samples spiked in this study (Boxplots) relative to the minimum theoretical uncertainty level achievable (grey lines).

3. Nobias pre-concentration protocol

The Nobias pre-concentration setup is displayed in Figure S4, rigid Teflon tubing is used to pump wash, samples and elution solutions reducing contamination risks between different samples. During washing and pre-concentration, waste are pumped via a Tygon tube connected at the bottom of the Nobias column through the same peristaltic pump in a parallel channel ensuring equal fluxes of 10ml.min^{-1} in and out of the column.

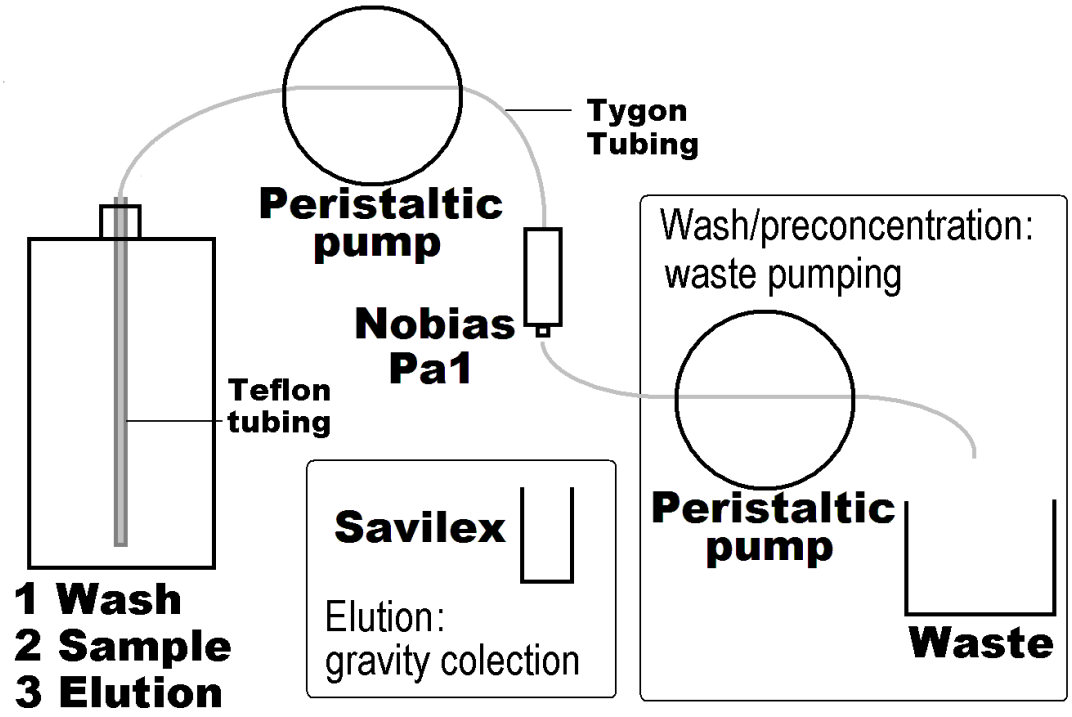

Figure S4: Nobias preconcentration setup

4. Oxides and mass bias monitoring solutions

The monitoring of Ba and REE oxides production were made analyzing two in house bracketing synthetic solutions of natural isotopic abundances (JMC solutions). One contains elements Ba, La, Ce, Pr, Tb and Er and the other Nd, Sm, Eu, Gd, Dy and Yb.

For La Ce and Lu mass bias fractionation factors were monitored by the analysis of bracketing mixed spike solutions. For other REE and Ba, mass bias was monitored with the two bracketing solutions Figure S5.

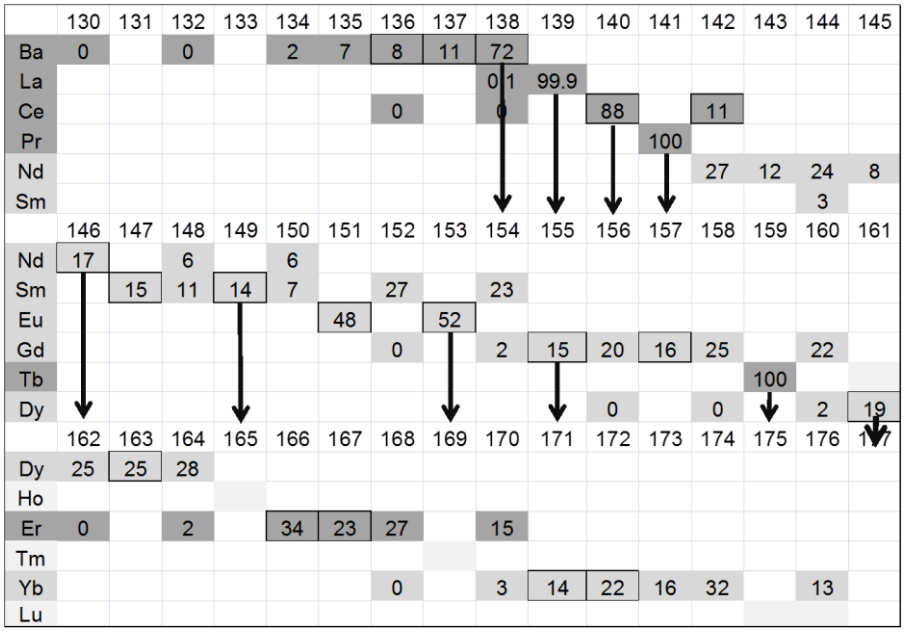

Figure S5: Two external bracketing solutions were used to monitor oxides formation and mass bias during a SF-ICP-MS session. The first solution contained Ba, La, Ce, Pr, Tb, Er (dark grey). The second solution contained Nd, Sm, Eu, Gd,Dy and Yb (light grey).Arrows point towards the monitored interfered masses, framed isotopes were used for mass bias monitoring.

5. Desolvator-SF-ICPMS settings and performances

5.1 Comparative test of two desolvator introduction systems

Ba and REE oxides formation were compared with two desolvation systems: the APEX-Q (ESI Inc.) with no N_2 additional gas and the Aridus II (Cetac Inc.) with N_2 as additional gas. The same monitoring solutions (ie: Ba, La, Ce, Pr, Tb, Er and Nd, Sm, Eu, Gd, Dy) were analyzed with both systems and displayed low oxides formation levels and a decreasing trend across the lanthanide serie with exception for Gd and Dy Figure S6. The best results were achieved with the Aridus II kept for the multispike method. The oxide formation levels presented here with this desolvation system corresponds to tuned values for UO/U of 0.02%.

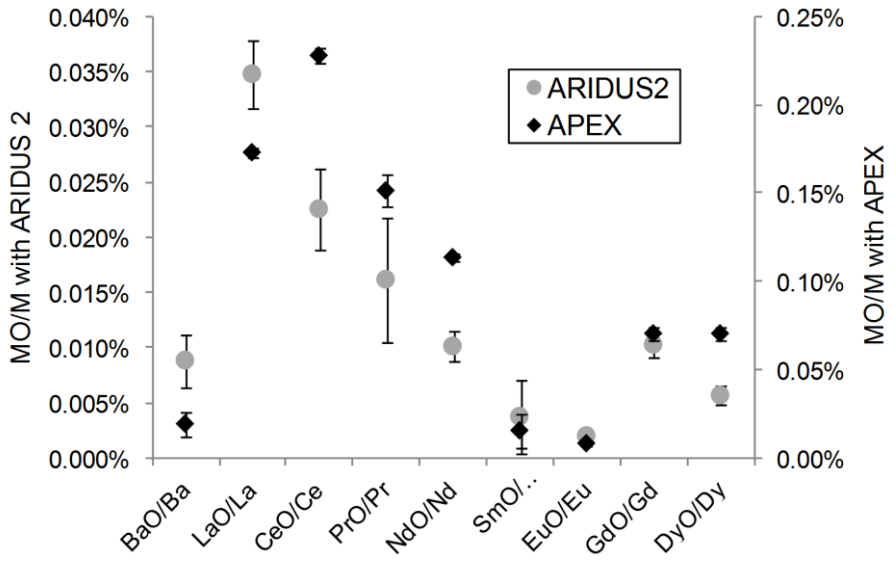

Figure S6: REE oxides formation in the Thermo Element XR ICPMS; comparison between ARIDUS 2 and APEX desolvating systems.

5.2 Comparative test of two data acquisition methods

For the multispike method we aimed in achieving the best precision on isotopic ratios. With traditional acquisition methods made of long measurements high precision are achieved on ion counting per masses, however small variations of the sample flow in the introduction system can lead to an increasing of RSD on isotope ratios measurements. As listed in Table S2, the 60 consecutive sweeps method displayed higher average RSD on individual measurements but lower 2RSD on isotopic ratios than a method constituted of 3 blocks of 3 long measurements.

Table S2: Comparison of standard deviation behavior on 5 replicate of single isotope analysis and isotopic ratios analysis for two different acquisition methods of same duration (n=5).

Acquisition method	^{143}Nd average RSD	^{146}Nd average RSD	143/146 2RSD ΔAmu=3	^{151}Eu average RSD	^{153}Eu average RSD	151/153 2RSD ΔAmu=2	^{172}Yb average RSD	^{173}Yb average RSD	173/172 2RSD ΔAmu=1
3*3 long meas.	1.6%	0.9%	**0.61%**	1.2%	0.8%	**0.71%**	0.9%	1.1%	**0.72%**
1*60 short meas.	1.7%	1.6%	**0.28%**	1.6%	1.5%	**0.31%**	2.1%	2.2%	**0.31%**

5.3 Desolvator-SF-ICPMS setup and configuration

The Table S3 lists the set up used for the multispike method, a wash time of 120s and a take up time of 90s allows the appropriate drop in the precedent sample inward and stabilization of the next sample signal.

Table S3: Instrument parameters

ICP system	
RF power, W	1200
Coolant argon flow rate, L min^{-1}	16
Auxiliary gas flow rate L min	1
Nebulizer gas flow rate L min	1.2
Sample introduction	
Sampler	
Peristaltic pump	3rpm
Nebulizer	GE Micromist TL 100µl
Sample uptake rate, µl.min^{-1}	260
Rinse time, min	4
Uptake time, s	120
Desolvation-system	
Desolvation-system	Aridus 2, membrane desolvation (CETAC)
Spray chamber temperature, °C	110
Membrane temperature, °C	160
Ar sweep gas l.min^{-1}	5.99
N_2 desolvation gas	12

Mass spectrometer	
Sampler	Nickel, orifice 1.0 mm
Skimmer Nickel,	orifice 0.7 mm
Torch position	X=4.90 Y=3.9 Z=−1.6
Extraction, V	−2000
Focus, V	−1200
X-deflection, V	2.5
Data acquisition	
Mass range, amu	129–178
Dwell time/mass, ms	0.04-0.4
peaks/mass	4
Number of scans	60
Total acquisition time	6min

6. Mass bias Monitoring

The average and standard deviation of 7 replicates of the measured/natural isotopic ratios of 8 elements monitored measured over the course of one analytical session are reported in Table S4. Details of the trends of 4 elements are represented in Figure S7. A comparison of using session averaged mass bias factors or interpolating evolutive mass bias factors shows that the final concentration results are within 0.1%.

Table S4: Average and standard deviation of the measured/natural isotopic ratios of the mass bias monitoring solution during one analytical session (n=7).

	142Ce/ 140Ce	146Nd/ 145Nd	149Sm/ Sm147	153Eu/ 151Eu	157Gd/ 155Gd	Dy163/ 161Dy	Er167/ 166Er	172Yb/ 173Yb
Rmes/ Rnat	1.009	1.013	1.007	1.014	1.008	1.009	1.001	1.011
Sd	0.002	0.002	0.004	0.004	0.001	0.003	0.003	0.007

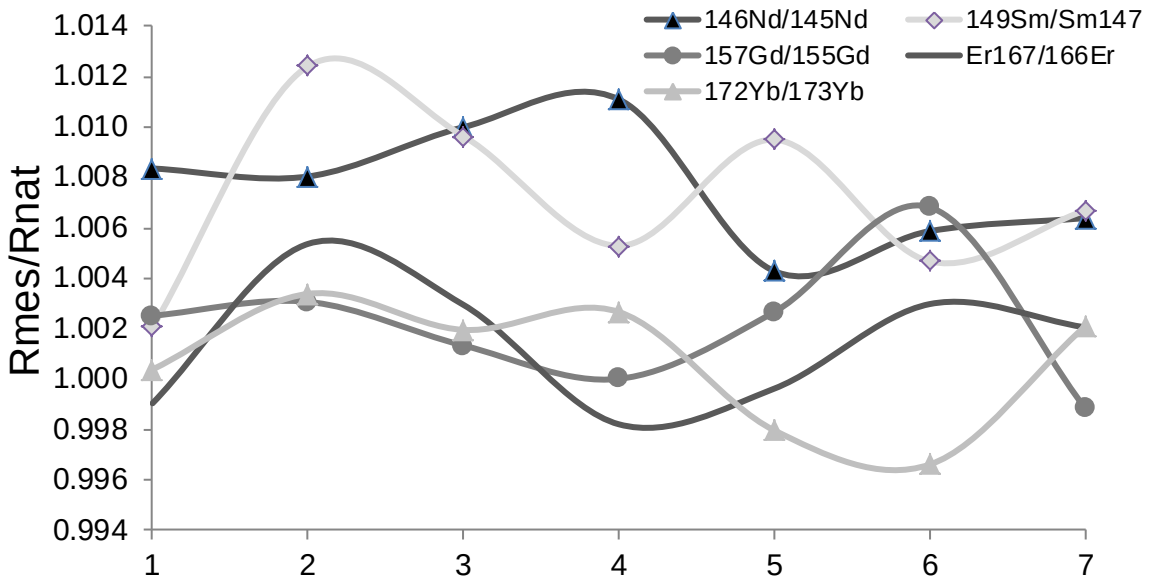

Figure S7: Mass bias evolution of Nd, Sm, Gd, Er, and Yb during one analytical session

7. Isobaric corrections on 138La and 176Lu

The linear relation between $^{138}Ce/^{140}Ce$ vs $^{136}Ce/^{140}Ce$ and $^{176}Yb/^{172}Yb$ vs $^{172}Yb/^{171}Yb$ is reported on Figure S8 and allows to subtract ^{138}Ce and ^{176}Yb interfering on La and Lu for any spike/sample proportion. The isobaric interference calculation is corrected for mass bias fractionation combining Eq 15 and 16 with Eq 17. (Eq. S15 and S16)

$$Cps^{138}La = Cps^{138} - \frac{Cps^{137}Ba}{A^{137}Ba} * \frac{A^{138}Ba}{f_{138/137}} - \left(\frac{Cps^{136}Ce*0.0305}{f_{136/140}} + 0.0028 * Cps^{140}Ce\right) * f_{138/140} \quad \text{(Eq.S15)}$$

$$Cps^{176}Lu = Cps^{176} - \frac{Cps^{177}Hf}{A^{177}Hf} * \frac{A^{176}Hf}{f_{176/177}} - \left(\frac{Cps^{171}Yb*0.909}{f_{171/172}} + 0.0101 * Cps^{172}Yb\right) * f_{176/172} \quad \text{(Eq.S16)}$$

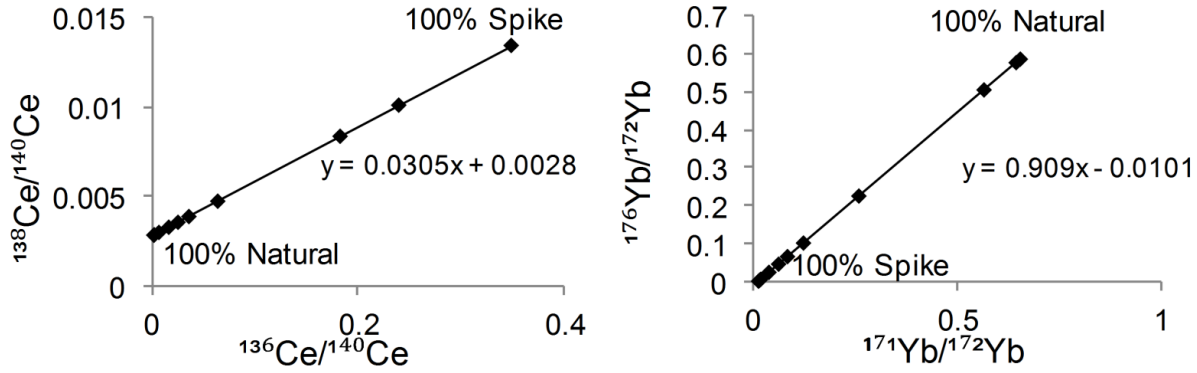

Figure S8: Isotope ratios of Ce and Yb for different proportions of spike/sample mixing.